Development of an Absolute Coordinate Calibration Device for Beam Profile Monitor

Ju-Hwan Yoon[1], Moses Chung[1*], Garam Hahn[2*]

[1]Department of Physics, Pohang University of Science and Technology (POSTECH), Pohang 37673, Republic of Korea.
[2]Pohang Accelerator Laboratory (PAL), Pohang 37673, Republic of Korea.

*Corresponding authors. E-mail(s): moses@postech.ac.kr; garam@postech.ac.kr;

Abstract

Beam profile monitors (BPRMs) based on fluorescent screen plates have been widely used in various accelerator facilities due to their intuitive structure and convenient camera-based readout system. However, calibration methods to correct complex measurement errors caused by factors such as the misalignment of screen, distance variations from the camera, and assembly tolerances with actuators have not yet been well developed. We have developed a device capable of performing an an absolute coordinate calibration for the beam image on the screen, using the ends of the beam pipe flange as reference points. This device consists of a two-axis motorized linear stage, two pairs of precision grid glass plates, a digital camera, and a BPRM chamber support. By utilizing geometrically well-aligned grid plates and a camera, we derived a method to get a perspective calibration matrix that maps the projected coordinates of the BPRM screen onto a 2D raster image. By applying this matrix, we were able to accurately obtain both the absolute central position and the shape of the beam in precise coordinates. In this paper, we will showcase the development process of the device, the numerical model, and the measurement results.

Keywords: Beam Profile Monitor, Scintillator Screen, Absolute Coordinates, Perspective Calibration

1 Introduction

The beam profile monitor (hereafter, BPRM) system is crucial for operating the accelerator by manifesting the qualitative image of the transverse beam. The parameters, including beam size, distribution, and intensity, are able to be obtained and analyzed [1, 2]. A beam diagnostics based on the scintillating screen has been notably adopted by reasons of its intuitive configuration and convenient buildability using the camera [3]. However, beam profile monitoring so far has not hitherto evaluated the beam image quantitatively. Usually, the two-dimensional qualitative and outlined image has been monitored to verify the beam. This type of image can reflect errors arising from equipment or measurement processes, making it challenging to accurately determine the precise properties of the beam. The elaborate monitoring of the beam emittance, shape, accurate distribution, and size is possible if the beam image can be quantitatively analyzed [4]. Thus, we will present the method of quantitatively investigating the beam profile by constructing an instrument that can set the absolute coordinates of the screen and capture it using a calibration camera as shown in Figure 2. Through this, the original shape of the beam can be obtained without distortion, enabling quantitative analysis of its properties.

One of the challenging parts of screen-camera monitoring is that no method currently exists to capture the beam profile images based on an accurate and flat spatial scale [5]. The diagnostic camera is mounted externally to the chamber and orthogonally to the beam path, the scintillating screen surface being projected obliquely to the camera [6]. Here, the arrangement of the screen and the precision of the device setup give rise to an aberration on the profile image acquired. One is the imperfect flatness of the image due to the variability in the distance between the camera and the screen inside the chamber because the arrangement of the screen changes whenever it is installed and inserted into the beamline [1]. The other is the assembly tolerance in the device components such as actuator, screen supporter, and chamber design, which interferes with measuring the absolute coordinates of the 2D beam profile with respect to screen position. To fix these drawbacks, zero-point calibration of BPRM equipment is required, along with the installation of a device capable of establishing the absolute coordinates of the screen. This enables more accurate numerical calculations for beam diagnostic images.

In this study, we will transform the distorted screen image into an accurate 2D image which embodies the original transverse beam profile. By extracting the desired point from the scintillating screen, it is not required to measure the screen size directly above its surface. A two-axis calibration stage newly developed by our group can control the motor of each axis in microunit meters, and the calibration camera captures the screen image on the specific positional coordinates. The accuracy of the camera position is verified by inspecting the linear alignment of the stage and the repeatability of the motor. The captured screen images are then transformed into a flat one using the perspective transformation, enabling the acquisition of undistorted 2D BPRM images of the scintillating screen [7].

We, in this paper, show the distribution and shape of the transverse beam can be transformed into its original, along with the quantitative profile value without distortion. Compared to the raw image of the oblique screen, the transformed images

more accord with the transverse beam profile. Collectively, this research showcases the method for acquiring absolute beam profile images, the numerical model of perspective transformation, and the establishment of the BPRM calibration stage.

2 Perspective Transformation Method

The method of transforming the coordinate space in accordance with the perspective aims to recasting homogeneous 2D profile image from distorted one [7]. Since the diagnostic camera catches the scintillating screen leaned, the resultant profile image is inevitably twisted, i.e., perspective distortion. We apply the perspective transformation method to restore the original transverse beam profile image like as it is seen from a viewpoint parallel to the beam. A perspective matrix has a linkage between the distorted plane and the corrected plane image. The matrix can be derived from the coordinates on each plane, thereafter remapping the coordinates of the distorted plane one by one [8]. The result of the transformation is, then, a flat image of the plane reconstructed from an existing misaligned image.

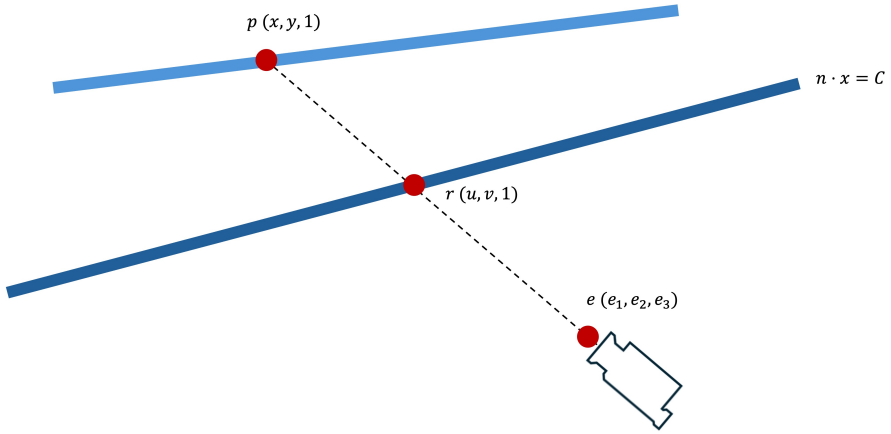

Fig. 1: An overview of the experiment stage capable of defining the transverse beam profile space.

A source plane observed by a camera, $\boldsymbol{e}$, is projected on the target plane which corresponds to the transformed image, C, namely $\boldsymbol{n}\cdot\boldsymbol{x} = C$. This pair of skewed planes is viewed by the camera, projecting one plane onto another. The relationship between two planes can be expressed by connecting each plane with a straight-line segment through the camera's viewpoint. The points where the line and the plane intersect are expressed as $\boldsymbol{p}$, and $\boldsymbol{r}$, respectively, where the projected point $\boldsymbol{r}$ of $\boldsymbol{p}$ is assumed to lie in the target plane, $\boldsymbol{n}\cdot\boldsymbol{x} = C$. Equation (1) represents how the points on each planes and the fixed coordinates of the camera as a line segment:

$$\boldsymbol{r} = (1-t)\boldsymbol{p} + t\boldsymbol{e}, \tag{1}$$

where t ranges from 0 to 1. t is a parameter that defines the line segment connecting two endpoints, and Eq. (1) can be rewritten as in Eq. (2) by combining with the plane equation $\boldsymbol{n} \cdot \boldsymbol{x} = C$.

$$\boldsymbol{r} = \frac{\boldsymbol{n} \cdot \boldsymbol{e} - C}{\boldsymbol{n} \cdot \boldsymbol{e} - \boldsymbol{n} \cdot \boldsymbol{p}} \boldsymbol{p} + \frac{C - \boldsymbol{n} \cdot \boldsymbol{p}}{\boldsymbol{n} \cdot \boldsymbol{e} - \boldsymbol{n} \cdot \boldsymbol{p}} \boldsymbol{e}. \tag{2}$$

Here, $\boldsymbol{r}$ and $\boldsymbol{p}$ can be represented as coordinates on the planes in the form of (u, v) and (x, y), and we can write Eq. (2) as the coordinate equation by expanding the equation for each coordinate. A perspective transformation is defined in this context, and the coordinates of two planes are related by the transform matrix.

A transformation matrix, also known as homography, conducts the transformation of the source coordinate space where an arbitrary coordinate (x_i, y_i) exists into the target coordinate space of (u_i, v_i) which portrays an orthographic 2D image. Equation (2) can be combined with the coordinate system represented as (x, y) and (u, v). Coefficients and constants are grouped together to be organized as in the following.

$$(u, v) = \left(\frac{ax + by + c}{gx + hy + j}, \frac{dx + ey + f}{gx + hy + j} \right). \tag{3}$$

The transformation matrix simplifies this relationship, enabling to connect all the coordinates in the plane.

$$w \begin{bmatrix} u_i \\ v_i \\ 1 \end{bmatrix} = \begin{bmatrix} a & b & c \\ d & e & f \\ g & h & j \end{bmatrix} \begin{bmatrix} x_i \\ y_i \\ 1 \end{bmatrix}, \tag{4}$$

where z-component is remained as 1 and the matrix is normalized to have $j = 1$ [9]. w is a scaling factor which expresses the extent of the perspective underlying on the points interested. Equation (4) is, then, rearranged into a simultaneous equation matrix in the form, $\mathbf{Ah} = 0$ to facilitate the calculation of the matrix elements.

$$\begin{bmatrix} x_i & y_i & 1 & 0 & 0 & 0 & -x_i u_i & -y_i u_i & -u_i \\ 0 & 0 & 0 & x_i & y_i & 1 & -x_i v_i & -y_i v_i & -v_i \end{bmatrix} \begin{bmatrix} a \\ b \\ c \\ d \\ e \\ f \\ g \\ h \\ j \end{bmatrix} = \begin{bmatrix} 0 \\ 0 \end{bmatrix}. \tag{5}$$

In this equation, the transformation matrix can be calculated through four pairs of coordinates which are randomly selected within the target space and the source space, respectively. The matrix relates the coordinates chosen with the coordinates on the source space. This serial process is repeated for all the coordinates, rectifying the distorted space into the flatten space which shows the transverse beam profile image.

Therefore, by applying a perspective transformation, the whole image can be adjusted using a homographic matrix, converting the tilted image into a planar one.

3 Experimental Setup

3.1 Configuration of the calibration stage

To calibrate and monitor the beam profile, we designed a BPRM device that allows to calibrate absolute coordinate spaces of the beam image on the scintillating screen. A key of this apparatus is that it enables us to capture the screen image remotely from a distant position outside the chamber without position deviation, and consequently acquire a 2D transverse beam image through the accurate coordinate points captured. Figure 2 illustrates a schematic of the screen monitor. It consists of a 1.6 Megapixel CMOS camera (acA1440-220 um, from Basler) for the 2D beam profile coordinates calibration, two-axis camera stage driven by the stepping motor, a pair of grid glass plates, and a scintillating screen such as a Ce:YAG single crystal, and the screen holder. We, first, installed a dummy chamber instead of the beam diagnostics chamber, so that grid plates are located at both ends of the chamber. The system was aligned such that the centers of the grids appeared to be collinear when viewed from the calibration camera.

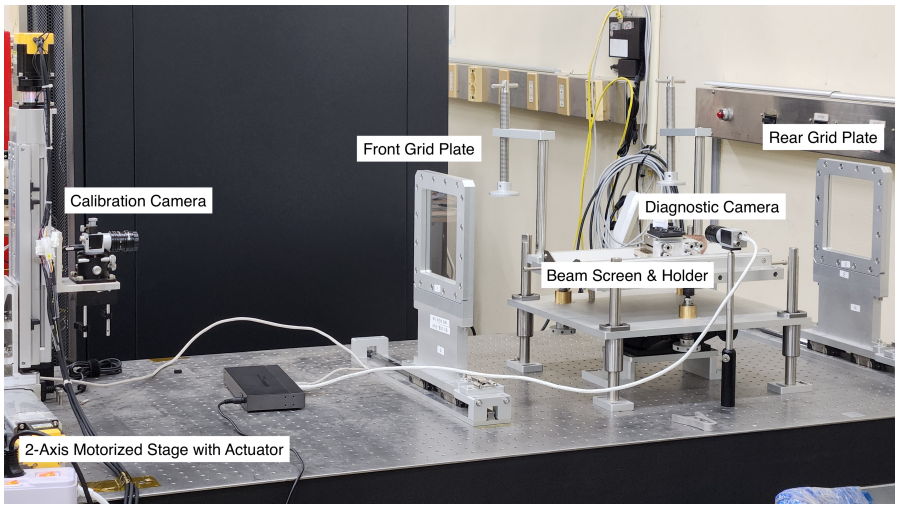

Fig. 2: An overview of the experiment stage capable of defining the transverse beam profile space.

There are two factors associated with motor performance: repeatability and positioning accuracy. We investigated the repeatability of the motor and confirmed the range of the misstepped value in the return-to-origin position. Moreover, we examined not only the alignment of the stage which includes the camera and screen holder but

also the grid glass plates which are crucial for calibrating the position of the calibration camera in beam monitoring. Immediately after inspecting the stage alignment, four arbitrary points on the screen were captured in accordance with the principle of perspective transformation. A Python code straightens up the distorted screen image, and the comparison of the rectified image and the original quantifies the image transformation accuracy [10].

3.2 Motor linearity

It is of importance to build BPRM stage feasible to detect the beam profile based on the accurate coordinate position [10]. However, the grid plate could not be perfectly operated since the actuator, the camera path, was not 100% straight as if the grid line was crookedly printed; an active area is assessed, moving the camera in both horizontal and vertical axes and checking whether the center of the camera and the grid intersection, i.e. coordinates, overlap at the same time. This alignment procedure was conducted for each of the two grid plates where the transverse beam coordinate space is defined and the camera can detect the screen. It enabled a measurement of how much the camera center deviates from the grid line at a specific point. This information allowed us to quantify the positional error in absolute coordinates—that is, the discrepancy between the expected grid location and the actual camera position—when the camera is moved to arbitrary positions within the coordinate space defined by the grid plates.

The two-dimensional coordinate space was mapped with the 5 mm units of the grid line, by which the active area was confirmed where the maximum appearing error can be evaluated in both the vertical and horizontal directions from the origin. We regulated the active area as the range of the grid plates, which corresponds to -70 mm to 70 mm in both the horizontal and vertical axis. Then, a tendency of the positional deviation depicted by the vector in Fig. 3 was interpolated by the 2D spline which showed the accurate position of the coordinates on the grid plate, reflecting the deviation of the motor. It modeled a global mapping of the motor's actual trajectory using grid points arranged at 5 mm intervals, thereby enabling precise calculation of the position of any arbitrary point inside a grid cell. Through this process, one can monitor the beam profile by installing the scintillator within the active area along with the completed alignment of the BPRM stage.

3.3 Motor repeatability

Additionally, we take into account the performance regarding the repeatability of the stepping motor on each axis — since the camera has to be positioned at specific points on the screen even after the repeated motion, the motor control plays a crucial role in determining the error of the BPRM images. Repeatability indicates whether the motor can return the camera position to its origin even after repeated motion to different coordinates, and no tolerance is allowed regarding the deviation of commanded and actual coordinates.

We inspected the repeatability by moving the calibration camera mounted on the sliding table. It conducted a set of motion programmed to move from the origin on

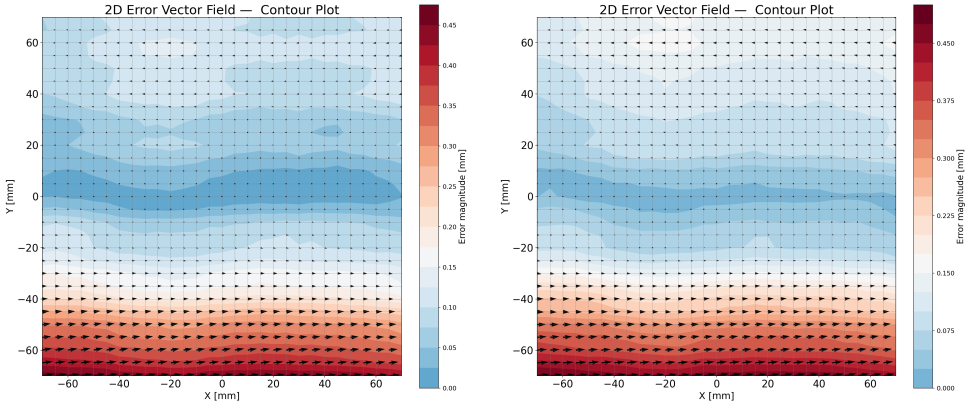

(a) (b)

Fig. 3: A result of the motor linearity test. (a) is the camera position error for all grid points of the front grid plate and (b) is for the rear grid plate. Vectors illustrate the deviation of the camera position on each grid and it is exaggerated to visualize the error. The contour plot on the background expresses the magnitude of the vector and both grid has similar distribution, meaning that the actuator of 2-axis stage definitely bends the camera position.

the central grid crossline, reach both endpoint 70 mm from the origin, and return to the origin point, while taking a picture whenever it finished one sequence. The length change between the image and grid center was measured during the 30 times repeatitive motions, which showed the deviation of the return position from the original starting point. It showed that the horizontal axis motor had the Root Mean Square (RMS) of 0.1103 μm and that of of 0.1167 μm for the vertical axis. This measurement implied that the camera can accurately target specific positions on the beam screen with a maximum repeatability error of 0.1606 μm, considering both axes.

4 Beam Profile Image Transformation

We have built a two-axis motorized stage so far, and we gather a calibrated 2D image of a tilted screen. Since the objective is to observe a profile such as a beam distribution, the validity of the image transformation method was verified using a 500 mW laser beam instead of an actual electron beam. The image is obtained via the procedure of fixing four pairs of coordinates on both the image seen from the diagnostic camera view and 2D transverse plane projected on the beam chamber cross section. The screen contains points squarely 20.0 mm distant, respectively, with the laser beam profile centered inside this range. As we have raised the issue of the perspective, the image space observed from the diagnostic camera does not coincide with the image

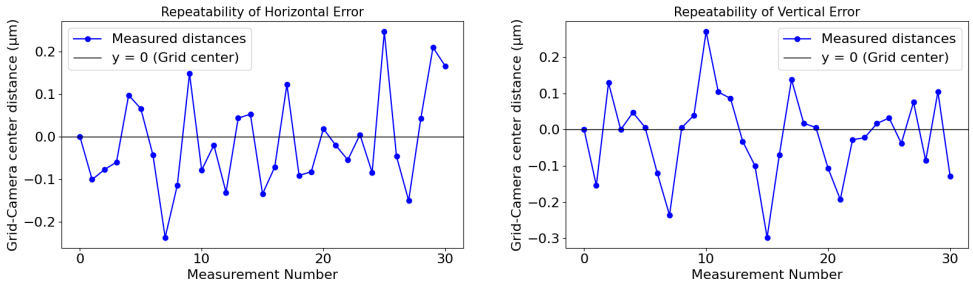

(a) Horizontal axis motor.

(b) Vertical axis motor.

Fig. 4: Results of the repeatability test of the two-axis motor. The variation in the difference between the camera center and the center of the grid lines was recorded after the one repeat motion. An offset was applied equal to the original data to use the original data as a reference.

projected onto the beam cross-section, resulting in discrepancy between the images. However, since four reference points can be identified in both images, a transformation matrix can be derived by relating their positions as captured on the tilted screen and as projected onto the beam cross-sectional image. Using this matrix, we demonstrated that the beam profile image can be transformed into the projected image showing the 2D transverse beam profile, regardless of how the mounted screen is tilted. The process was conducted through the image transformation Python code which applies perspective transformation to the input image. Then, the accuracy of the transformation was evaluated by comparing a transformed 2D beam profile image with the original 2D image.

The comparison of the transformed beam profile image and the accurate 2D transverse image validated the method of perspective calibration based on coordinate calibration. According to the Figure 5, we analyzed the difference between two images via the normalized pixel intensities to minimize the background offset and rescaled pixel space to tune to the same position of the beam core. The vertical components had high accuracy of the beam profile, meaning that there were little distortion or expansion along the vertical profile. On the other hand, the horizontal components of the transformed image had wider distribution than that of the 2D accurate image. It resulted from the stretched transformation for the image captured by the diagnostic camera.

The main source of the error is the digitization limit in coordinates selection on the beam screen. We selected four reference coordinates on the beam screen from both the diagnostic camera image and the corresponding 2D planar projection. However, due to the resolution limitations of both images, it was not possible to select precisely exact same positions. Besides, the optical system, such as the lens abberation or unnecessary image noise, can invoke the additional bias.

The mechanical error in the calibration stage, particularly the motor, is summarized into two primary sources of error in estimating the coordinates of the beam

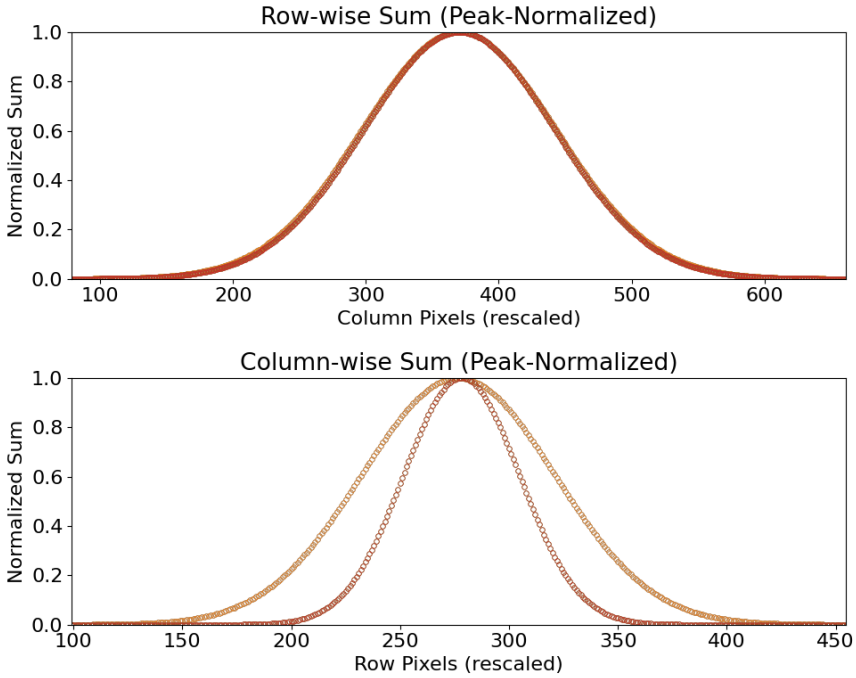

Fig. 5: Comparison of the perspective-transformed image (Orange) and the 2D transverse beam image (Red) profiles. The beam profile distribution was obtained by summing the pixel intensities along the horizontal and vertical directions of each image.

profile image. The first is the image position analysis error $\sigma_{\text{linearity}}$, which arises from the inability to precisely identify the coordinates within the image. There is a quantitative measurement limitation (measurement resolution) imposed by the pixel size, and the minimum measurable unit determined by the equipment used in this experiment was found to be 0.526 μm. The second is the motor precision error $\sigma_{\text{repeatability}}$ due to the repeatability limitations of the two-axis camera stage. It was 0.1606 μm as mentioned before, which contains both the horizontal and vertical error. Assuming these two errors are independent, the total coordinate measurement error can be approximated as follows:

$$\sigma_{\text{total}} = \sqrt{\sigma^2_{\text{repeatability}} + \sigma^2_{\text{linearity}}} \tag{6}$$

Albeit the image is perfectly transformed, the inbuilt uncertainty of the image is σ_{total}, 0.550 μm, in which the repeatability error has a relatively small value compared to the linearity one. This combines with the image transformation flaw due to the relatively inaccurate collection of the coordinates which is the boundary condition for the perspective transformation. Thus, independent of the BPRM stage errors, these uncertainties arise from the image coordinates extraction process and can introduce minor

inaccuracies into the transformed images. Nevertheless, we corrected the perspective distortion which is inevitable in diagnostic equipment based on the scintillating screen image. In the range of the available 2D transverse beam area, we can define the coordinate space and find the relationship between it and the image obtained by the diagnostic camera.

5 Conclusion

Taken together, the 2D transverse beam profile is required to study the characteristics of the beam based on the measurable data. We obtained the beam profile by taking advantage of the BPRM stage which can calibrates the measurement errors and target the absolute coordinates. In the measurement process, there was instrument error such as the repeatability misstep of the camera movement motor and the misaligned linearity in the 2D coordinate space. While the comprehensive resolution of the error was calculated as 0.550 μm, the accurate coordinates were figured out through interpolation between the motor's readout positions and the actual coordinates marked on the grid surface. The perspective transformation reshaped the slanted image space into the transverse one, which was followed by the assessment of of the accuracy of the image perspective transformation. This was conducted by comparing the transformed images to the original images projected onto the beam cross-sectional plane. Although some discrepancies were observed in the horizontal profile compared to the vertical profile, the overall image demonstrated that the image captured by the diagnostic camera can be remapped onto the 2D plane, calibrating the positional deviation generated by the two-axis motor stage and its performance. In the future, we expect that the improvement in the noise removal and resolution limits inherent in the image will enable the acquisition of more detailed profiles, and that refining the coordinate assignment method used as boundary conditions will help reduce errors in image transformation.

Acknowledgements. This work was supported by the National Research Foundation of Korea (NRF) funded by Ministry of Science and ICT under Grant 2022M3I9A1073808.

References

[1] Kang, X., Tang, K., Li, Y., Zhao, T., Mao, R., Li, M.: Development of a water-cooled scintillation screen for high-current beam profiling. Journal of Instrumentation **19**(10), 10001 (2024)

[2] Najafiyan, A., Abbasi, F., Hajari, S.S., Ghasemi, F.: Beam Profile Monitor Design for a Multipurpose Beam Diagnostics System

[3] Walasek-Höhne, B., Kube, G.: Scintillating screen application in beam diagnostics. In: Proceedings of DIPAC, p. 553 (2011)

[4] Hashimoto, Y., Muto, M., Norimura, K., Watanabe, K.: Beam profile monitor using alumina screen and CCD camera. Technical report, Tokyo Univ. (1992)

[5] Yamada, I., Wada, M., Moriya, K., Kamiya, J., Saha, P.K., Kinsho, M.: High-intensity beam profile measurement using a gas sheet monitor by beam induced fluorescence detection. Physical Review Accelerators and Beams **24**(4), 042801 (2021)

[6] Koziol, H.: Beam diagnostics for accelerators. Technical report, CERN-PS-2001-012-DR (2001)

[7] Austin, D.: Using Projective Geometry to Correct a Camera. American Mathematical Society (2013)

[8] Bevilacqua, A., Gherardi, A., Carozza, L.: Automatic perspective camera calibration based on an incomplete set of chessboard markers. In: 2008 Sixth Indian Conference on Computer Vision, Graphics & Image Processing, pp. 126–133 (2008). IEEE

[9] Heckbert, P.S.: Fundamentals of texture mapping and image warping. Citeseer (1989)

[10] Braccini, S., Carzaniga, T.S., Casolaro, P., Dellepiane, G., Franconi, L., Mateu, I., Scampoli, P., Schmid, M.: A two-dimensional non-destructive beam monitoring detector for ion beams. Applied Sciences **13**(6), 3657 (2023)